

Mechanical Properties and Bonding Mechanisms of Carbonated Recycled Fine Aggregates (RFA) with Industrial Wastes

Huan He, Zhexion Liu, Man Li

Institute of Geotechnics, Southeast University, China, h_he@seu.edu.cn

Jing Ren

Nanjing Institute of Technology, China

ABSTRACT: Landfilling industrial and demolition waste consumes land and poses environmental risks. To address this while promoting carbon reduction and resource efficiency, this study investigates CO₂ activation of such waste to produce a novel carbonated paste for geotechnical and road applications. A reactive matrix of magnesium slag (MS), fly ash (FA), and MgO was blended with recycled aggregate fines (RAF) as a structural skeleton to enhance carbon sequestration. Physical and mechanical properties were evaluated under carbonation curing, with standard curing as a reference. A 3-day carbonation process significantly activated MS, increasing strength up to 12.3 times compared with standard curing (4.9 MPa vs. 0.4 MPa). Prolonged carbonation achieved a maximum strength of 13.52 MPa. Reaction mechanisms were analyzed through pH, conductivity, quantitative X-ray diffraction, thermogravimetric analysis, and scanning electron microscopy. The main strength-contributing products—Nesquehonite, Dypingite, Magnesite, and Calcite—formed via carbonation of MgO, MS, and RAF. A porous structure was essential for CO₂ diffusion and reaction. The water-to-cement (W/C) ratio, calcium-to-magnesium (C/M) ratio (MS:MgO), and porous FA particles critically influenced internal pore volume, thereby affecting strength. These findings demonstrate the synergistic use of CO₂ and alkaline industrial waste to create sustainable construction materials, offering a pathway for carbon capture and waste valorization.

KEYWORDS: Paper template, instructions.

1 INTRODUCTION

The emissions of greenhouse gases, particularly CO₂, are major contributors to global warming, with 33–40% of anthropogenic CO₂ from fossil fuel combustion (Liu et al., 2024). Global fossil fuel CO₂ emissions reached 37.9 Gt in 2021, primarily from power, industry, transport, and buildings (Crippa et al., 2022). Carbon capture, storage, and utilization (CCSU) is a key mitigation strategy, potentially reducing CO₂ emissions by 14% by 2050 (IEA, 2023). Among CCSU options—geological, ocean, biological, and mineralization—mineral storage is considered safest and most feasible. Alkaline industrial wastes such as fly ash (FA) and magnesium slag (MS) are highly reactive to CO₂ and more cost-effective than natural minerals (Liu et al., 2021; Pan et al., 2020), enabling simultaneous carbon capture and waste reduction.

The Pidgeon process generates 5.5–10 t MS per t magnesium metal, with annual accumulation rising. MS contains high γ -C₂S and *f*-CaO, offering low-carbon potential despite limited direct use. MS-based carbonate binders have reached >100 MPa compressive strength but require high-pressure or high-CO₂ curing. Reactive MgO offers rapid strength development under carbonation, but its high cost limits application. FA improves binder flowability and carbonation depth due to its spherical, porous morphology. Combining MS and FA in MgO-based binders may reduce cost, increase waste utilization, and enhance carbonation efficiency. However, mechanisms under simultaneous hydration and carbonation remain unclear due to complex ion interactions and pore structure evolution.

Cement production contributes 5–7% of global anthropogenic CO₂ emissions. Recycling demolished cement products, especially recycled aggregate fines (RAF), can reduce emissions. RAF, often discarded due to poor grading and low strength, mainly consists of hydrated cement clinker with notable CO₂ capture potential. Small RAF particles (<0.15 mm) show highest reactivity in wet carbonation, and carbonated

RAF can improve cement paste properties and serve as a supplementary cementitious material. Methods such as semi-dry, mechanochemical, and pH cycling carbonation can activate RAF but are often energy-intensive or produce secondary waste.

This study develops a carbonate binder of MgO, MS, and FA, incorporating RAF as a skeleton to enhance carbon sequestration and C&D waste utilization. The effects of binder composition, curing conditions, and water-to-cement ratio on flowability and mechanical properties are assessed. Carbonation mechanisms are examined via pH, conductivity, QXRD, SEM-EDS, and TGA, while BSED-EDS characterizes microstructural porosity to elucidate factors controlling carbonation rate.

2 MATERIALS AND METHODS

2.1 Materials

The recycled aggregate fines (RAF) used in this study were sourced from a renovation project in Qinhuai District, Nanjing, containing debris such as red bricks and waste glass. Following Jiang et al. (2022), RAF <150 μ m exhibit high carbonation reactivity; thus, recycled fine aggregates (<4.75 mm) were crushed and sieved to <0.15 mm, yielding yellowish-brown particles (peak size 148 μ m) with variable shapes. Fly ash (FA), a Class 1 product (GB/T 1596-2017) from Huadian Group, is black, predominantly spherical, and smooth-textured, with a peak size of 104.7 μ m. Magnesium slag (MS) from Anhui Chao Lake Yunhai Magnesium Industry Co., Ltd., produced during magnesium smelting, is gray, layered, and fine (37 μ m peak size) due to high γ -C₂S content. Magnesium oxide (MgO) from Hebei Longxing Co., Ltd. is white, crystalline, and highly reactive (68.58% active MgO), with a peak size of 31 μ m. A small amount of polycarboxylic acid-based superplasticizer from FuClear Co. was also used.

2.2 Mix design

The experimental design and mix proportions (Table 1) used a carbonate binder of MS, MgO, and FA, with RAF as a skeleton to enhance carbon sequestration. Optimal binder ratios were determined via a simplex centroid mixture design (Minitab 19, trials No. 1–10), where the mass fractions of MS, MgO, and FA totaled 1 (each 0.1–0.8). RAF-to-binder ratio was fixed at 1:2.

Table 1 Experimental designs for the current study.

| Sample code | R A F | F A | M S | M gO | S P | W/C ratio | Curing time |
|-------------|----------|-----|-----|------|-----|-----------|-------------|
| NO. 1 | 0.5 | 0. | 0. | 0.8 | | | |
| | | 1 | 1 | | | | |
| NO. 2 | 0.5 | 0. | 0. | 0.4 | | | |
| | | 45 | 1 | 5 | | | |
| NO. 3 | 0.5 | 0. | 0. | 0.3 | | | |
| | | 33 | 33 | 3 | | | |
| NO. 4 | 0.5 | 0. | 0. | 0.1 | | | |
| | | 1 | 8 | | | | |
| NO. 5 | 0.5 | 0. | 0. | 0.2 | | | S14, |
| | | 56 | 22 | 2 | | | C3+S11 |
| NO. 6 | 0.5 | 0. | 0. | 0.1 | / | 0.6 | or C7+S7 |
| | | 45 | 45 | | | | |
| NO. 7 | 0.5 | 0. | 0. | 0.2 | | | |
| | | 22 | 56 | 2 | | | |
| NO. 8 | 0.5 | 0. | 0. | 0.1 | | | |
| | | 8 | 1 | | | | |
| NO. 9 | 0.5 | 0. | 0. | 0.5 | | | |
| | | 22 | 22 | 6 | | | |
| NO. 10 | 0.5 | 0. | 0. | 0.4 | | | |
| | | 1 | 45 | 5 | | | |
| NO. 11 | 0.5 | 0. | 0. | 0.2 | / | 0.5 | |
| | | 22 | 57 | 2 | | | |
| NO. 12 | 0.5 | 0. | 0. | 0.2 | 0. | 0.4 | S14, |
| | | 22 | 57 | 2 | 5 | | C3+S11, |
| NO. 13 | 0.5 | 0. | 0. | 0.2 | 1 | 0.3 | C7+S7 |
| | | 22 | 57 | 2 | | | or C14 |
| NO. 14 | 0.5 | 0. | 0. | 0.2 | 1. | 0.2 | |
| | | 22 | 57 | 2 | 5 | | |

The water-to-cement ratio (W/C) was set at 0.6—higher than the typical 0.5—to maintain workability, as high MgO contents reduce flowability.

Curing lasted 14 days under four conditions: (1) standard curing (S14), (2) 3-day carbonation + 11-day standard curing (C3+S11), (3) 7-day carbonation + 7-day standard curing (C7+S7), and (4) 14-day carbonation (C14). This allowed assessment of hydration and carbonation contributions to strength, as both occur simultaneously during carbonation curing. Reaction products under each condition were analyzed to elucidate hydration–carbonation mechanisms.

2.3 Sample preparation

Dry powders were blended in an electric mixer, water added, and the paste mixed thoroughly. Flowability was tested per GB/T 8077-2023 using a truncated cone mold. The paste was cast into 40 × 40 × 40 mm molds, vibrated to remove air, and cured for 24 h in a standard chamber before demolding.

Specimens were then carbonated in 20% CO₂ at 75% RH and 20 °C for 0–14 days, followed by standard curing, with total curing set at 14 days. Four parallel specimens were prepared per mix, one for carbonation depth. Standard curing maintained >95% RH at 20 ± 2 °C.

3 RESULTS AND DISCUSSION

3.1 Mechanical properties

The compressive strength (UCS) results under various curing conditions are shown in Figure 7d. Under standard curing, UCS exhibited a positive correlation with MgO content and a negative correlation with FA content, differing from the optimal MgO dosage effect reported for MgO-activated GGBS systems (Jin et al., 2015; Yi et al., 2014). Increasing MS content also enhanced strength, but the effect was far less significant than MgO. At similar dry densities, mixes with higher MgO content (e.g., NO. 1, 1347 kg/m³, 2.8 MPa) consistently outperformed those with higher MS content (e.g., NO. 4, 1355 kg/m³, 0.4 MPa), confirming the limited contribution of MS hydration to strength.

An exception occurred in the mix with an MS:FA ratio of 1:1 and relatively low MgO content (NO. 6), where severe expansion led to specimen disintegration before demolding. While C. Zhang et al. (2023) attributed similar behavior in MS to *f*-CaO hydration expansion, in this study it is more likely due to the alkali–silica reaction (ASR) between FA and the alkaline environment generated by MS hydration. Because MS has low calcium content, Ca²⁺ is rapidly consumed in C–S–H formation, leaving excess OH[−] to react with SiO₂ in FA, producing ASR gel and associated volumetric expansion (Kim et al., 2015).

Carbonation curing markedly improved UCS compared to standard curing, especially in high-MS mixes. In NO. 4 (80% MS), UCS after carbonation was 11 times higher than under standard curing, far exceeding the 4.6-fold increase in NO. 1 (80% MgO). This demonstrates carbonation’s strong ability to activate MS and improve strength. The high-MS group also reached a strength plateau after 3 days of carbonation, highlighting MS’s rapid carbonation kinetics. Unlike MgO, whose carbonation causes more pronounced expansion that can block CO₂ ingress, MS carbonation preserves pore space, facilitating further CO₂ transport.

Interestingly, dry density changes did not consistently align with strength gains. For example, NO. 9 had the highest dry density (1563 kg/m³) but not the highest strength (5.7 MPa). Similarly, NO. 2 had a far greater density increase (157 kg/m³, 4.3 MPa) than NO. 10 (64 kg/m³, 4.5 MPa), yet their strength increments were comparable. This lack of direct correlation suggests that microstructural and mineralogical characteristics of carbonation products, rather than density alone, play a decisive role in strength development.

These findings underscore that while MgO remains a strong contributor to early-age strength through hydration and carbonation, MS offers significant benefits under carbonation curing, particularly in rapid early strength gains without severe pore blockage. However, FA content must be carefully controlled in MS-rich binders to avoid ASR-related expansion. The divergence between dry density and strength further

emphasizes the need to study carbonation product formation and pore structure evolution in detail to fully understand and optimize strength development mechanisms in such blended binders.

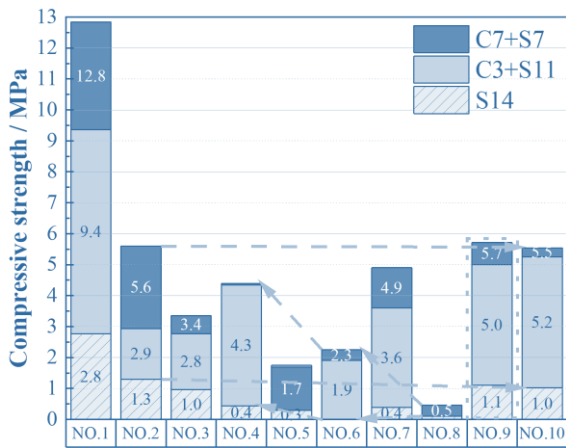


Figure 1. Compressive strength of the samples

3.2 Fluidity

Figure 5 shows the fluidity of fresh pastes (W/C = 0.6) with different mix ratios. Fluidity decreased markedly with increasing MgO content, consistent with previous findings for MgO–cement blends (Liu et al., 2024). At 80% MgO, the paste exhibited minimal spread after cone removal, resembling clay in its plasticity. This is due to the high purity and rapid reactivity of MgO, which hydrates quickly, consuming free water and reducing particle lubrication (Mo et al., 2010). The expansive nature of MgO hydration further fills voids between unhydrated particles, creating interconnections that restrict particle movement (Dung and Unluer, 2016).

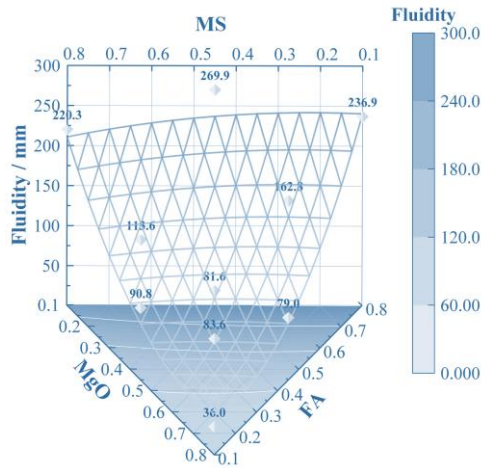


Figure 2. Fluidity of the samples

In contrast, higher FA content slightly improved fluidity, likely because the spherical FA particles promote particle mobility and reduce interparticle friction (Dung et al., 2020). Overall, satisfactory fluidity (GB/T 8077-2023: >120 mm) was achieved when MgO content was kept below 30% of the binder and 20% of the total paste.

3.3 Dry density

Figure 6d illustrates the effect of curing conditions on paste dry density. Under standard curing, dry density decreases with increasing FA content due to its low self-hydration, though the

reduction is smaller at low FA contents (0.1–0.2) as dissolved FA reacts with Ca^{2+} and Mg^{2+} to form hydrated aluminosilicates (Sun et al., 2022). For the same FA content, increasing MgO slightly raises dry density more than MS, reflecting MgO's higher reactivity (Mu et al., 2019).

Under combined carbonation curing, dry densities increased relative to standard curing, generally correlating with carbonation duration, except in high-MS mixes (>56%, NO. 4 & NO.7), where C7+S7 exhibited slightly lower density than C3+S11. This indicates controlled carbonation can enhance dry density in certain compositions, likely by promoting release of reactive components through pH reduction (Zhang et al., 2023).

FA content strongly influences carbonation-driven density changes. When FA exceeds 56%, the limited reactive component reduces the dry density gain; decreasing FA enhances the density increase (NO.8 → NO.6 → NO.4). Conversely, below 45% FA, further reduction lowers the density gain due to the reduced porosity needed for CO_2 transport, a behavior also noted in MgO-based cements (Liu et al., 2024).

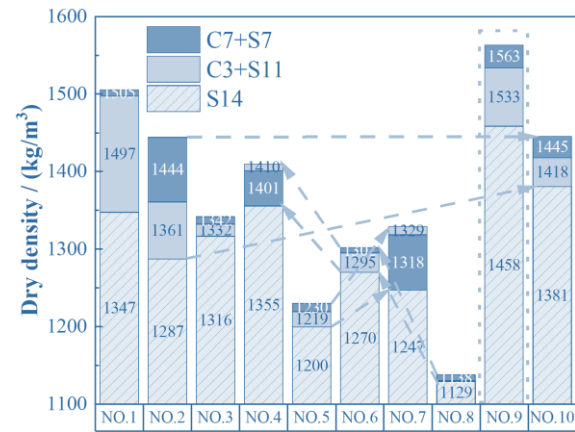


Figure 3. Density of the samples

3.4 Effect of dry density and moisture content on compaction strength

Figure 4 shows the dry density and moisture content of carbonated pastes with different W/C ratios. Moisture content decreases most rapidly during the first 0–3 days, dropping to 10.7–14.0%, then slows and stabilizes at 8.3–10.3% by day 14. Higher W/C pastes lose moisture faster due to greater porosity. Reduced moisture limits ongoing carbonation, explaining the smaller dry density and strength gains after 3 days.

Under standard curing, lower W/C ratios generally yield higher dry densities, though the relationship is affected by air entrainment from superplasticizer. For $\text{W/C} \geq 0.3$, dry density changes correlate with phenolphthalein test results for carbonation depth. However, the test cannot fully indicate carbonation completion; for example, in the 0.4 W/C sample, dry density continues to increase up to 14 days despite no phenolphthalein color change, showing that carbonation persists.

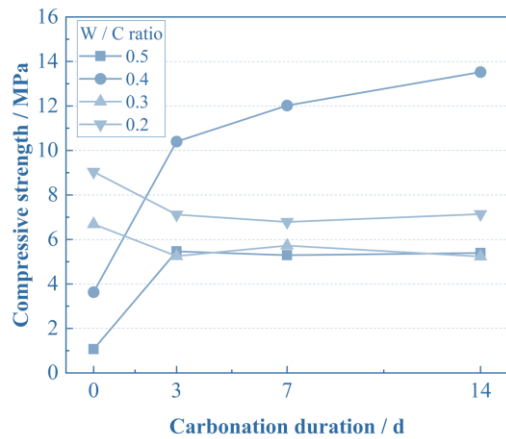


Figure 4. Changes in compressive strength with carbonation duration

3.5 Compound quantification via TGA

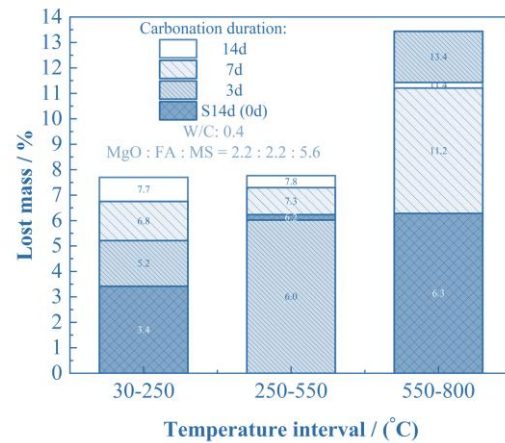
Thermogravimetric analysis (TGA) was conducted on pastes with an optimal W/C ratio of 0.4 to quantify products formed during carbonation. Mass loss in the 0–800°C range was divided into three intervals to distinguish contributions from different phases: 30–350°C (dehydration of C–S–H and hydromagnesite), 250–550°C (dehydroxylation of brucite and decarbonation of magnesium carbonates), and 550–800°C (decarbonation of calcite and magnesian calcite).

Under standard curing, mass loss in 30–250°C was low (3.4%), reflecting limited γ -C₂S hydration. The 250–550°C range showed 6% mass loss, mainly from brucite dehydroxylation, indicating near-complete MgO hydration (MgO = 14.67% of paste; H₂O:MgO = 18:40). Mass loss in 550–800°C was due to calcite from RAF.

After carbonation, mass loss increased across all intervals. In 30–250°C, dehydration of hydromagnesite rose with carbonation time, indicating enhanced formation and crystallinity. In 250–550°C, mass loss reflected both brucite dehydroxylation and magnesium carbonate decarbonation. Full carbonation of brucite would yield ~16.14% mass loss, yet even after 14 days only 7.8% was observed, suggesting incomplete conversion of Mg²⁺ to magnesium carbonates.

In 550–800°C, mass loss corresponded to decarbonation of magnesian calcite and calcite; overlapping decomposition temperatures prevented precise quantification. Interestingly, mass loss after 3 days of carbonation exceeded that after 7 or 14 days, indicating short-term carbonation promotes magnesian calcite formation, while longer carbonation favors hydromagnesite formation. These results highlight that carbonation reactions continue even after phenolphthalein tests indicate no further change, emphasizing the method's limitations in capturing ongoing carbonation.

Overall, TGA demonstrates that carbonation selectively alters mass loss across temperature ranges, reflecting the formation sequence and relative proportions of hydromagnesite, magnesium carbonates, and calcite in the paste.



4 CONCLUSIONS

This study demonstrates that binder composition and curing conditions critically influence the mechanical, physical, and chemical properties of MgO–MS–FA–RAF pastes. Under standard curing, compressive strength correlates positively with MgO content and negatively with FA, while MS contributes minimally. Carbonation curing markedly enhances strength, especially in high-MS mixes, due to rapid MS carbonation and preservation of pore space for CO₂ transport. Fluidity decreases with increasing MgO but improves slightly with FA, and satisfactory workability is achieved when MgO remains below 30% of the binder. Dry density increases with carbonation, influenced by FA content and reactive component availability, while moisture reduction governs carbonation progression. TGA confirms selective formation of hydromagnesite, magnesium carbonates, and calcite, highlighting that carbonation continues beyond phenolphthalein indications. Overall, optimizing mix ratios and carbonation conditions enables effective strength development, densification, and CO₂ utilization in these blended binders.

5 ACKNOWLEDGEMENTS

The work described in this paper was fully supported by grants from the National Natural Science Foundation of China (Grant No. 52478331).

6 REFERENCES

- Liu, W., Teng, L., Rohani, S., Qin, Z., Zhao, B., Xu, C.C., Ren, S., Liu, Q., Liang, B., 2021. CO₂ mineral carbonation using industrial solid wastes: A review of recent developments. *Chem. Eng. J.* 416, 129093.
- Liu, Y., Wang, B., Fan, Y., Yu, J., Shi, T., Zhou, Y., Song, Y., Xu, G., Xiong, C., Zhou, X., 2024. Effects of reactive MgO on durability and microstructure of cement-based materials: Considering carbonation and pH value. *Constr. Build. Mater.* 426, 136216.
- Liu, Z., Li, M., He, H., Ren, J., Liu, S., Zhang, X., 2025. Mechanical properties and reinforcing mechanisms of coupled-carbonated recycled fine aggregates (RFA). *Acta Geotech.*
- He, H., Senetakis, K., 2016. A study of wave velocities and poisson ratio of recycled concrete aggregate. *Soils Found.* 56(4), 593-607.
- He, H., Senetakis, K., Coop, M.R., 2018. Stiffness of a recycled composite aggregate. *Soil Dyn. Earthquake Eng.* 110, 185-194.
- He, H., Zhang, C., Yang, J., Li, M., Fu, W., Senetakis, K., Zhang, D., Liu, S., 2023. Characterization of recycled concrete aggregate (RCA) particles for geotechnical engineering applications: Particle strength and interparticle contact behavior. *Constr. Build. Mater.* 407, 133532.